Proceedings of CONF-MSS 2026 Syposium: Mechanical Control and Automation
DOI: 10.54254/2755-2721/2026.BJ32616

Inertia Evaluation and Optimization in Power Systems with High Proportions of Asynchronous Power Sources

Binghong Lin[1*], Zheng Jiang[1]

[1]*School of Energy and Electrical Engineering, Chang'an University, Xi'an, China*
**Corresponding Author. Email: 2023905154@chd.edu.cn*

Abstract. This paper focuses on the problem of power system inertia decline caused by changes in the composition and form of system inertia in power systems with a high penetration of non-synchronous power sources. Aiming at the scenario of high penetration of non-synchronous power sources, this paper expands the concept of synchronous generator inertia, proposes the inertia support characteristics of wind and photovoltaic power sources, and defines the composition and connotation of the equivalent inertia of the power system. Taking the IEEE 3-generator 6-node system with a high penetration of new energy (including photovoltaic and wind power) as a case study, the paper conducts optimal power flow calculation and unit commitment calculation, and then completes the system inertia evaluation. The research verifies the reliability of the proposed scheme, which effectively improves the equivalent inertia of the system, and provides theoretical support for the inertia regulation and operation optimization of new power systems.

Keywords: Power system inertia, Inertia decline, Inertia evaluation.

1. Introduction

As fossil fuels deplete and carbon emission regulations tighten, global energy pressure intensifies. Developing renewable energy (mainly wind and solar) is a global consensus. With more renewable energy integrated via power electronic converters, asynchronous power sources can no longer provide active inertia support, reducing power system inertia gradually.

Scholars worldwide have studied power system inertia demand and low-inertia issues from high renewable penetration. Literature [1] focuses on doubly fed induction generators, derives the equivalent virtual inertia time constant from maximum power curves and actual wind conditions, analyzes inertia characteristics, and proposes a medium-to-long-term prediction method. Literature [2] introduces System Inertia Requirement (SIR), presents an evaluation method and hierarchical mechanism to ensure frequency stability via multi-stage inertia support, providing a theoretical basis for precise inertia regulation. Literature [3] addresses multi-inertia-resource coordination in new power systems; considering their techno-economic features and constraints (frequency variation rate, minimum frequency), it establishes an operation cost minimization objective function and optimized scheduling schemes to reduce total system cost. Literature [4] defines generalized inertia (rotational and simulated) for new power systems, details four evaluation methods, and compares their advantages, applicable scenarios and objects.

© 2026 The Authors. This is an open access article distributed under the terms of the Creative Commons Attribution License 4.0 (https://creativecommons.org/licenses/by/4.0/).

DOI: 10.54254/2755-2721/2026.BJ32616

Based on power system inertia definition, this paper clarifies the composition and meaning of inertia in high-asynchronous-power systems. Optimal power flow calculation is performed on the IEEE6 node system, and inertia evaluation of results verifies the optimization scheme's reliability.

2. Establishment of system equivalent inertia model

2.1. Definition of inertia of power system

Inertia is an object's inherent property, manifesting as resistance to motion state changes, measured by mass. To ensure stable power system frequency control, its inertia evaluates AC grids' ability to maintain their original operating state.

2.2. Inertia constant of traditional power system

In traditional power systems, inertia mainly comes from rotational components (synchronous generators, asynchronous motors); adjusting their speed regulates grid frequency to achieve primary and secondary frequency modulation.

The concept of inertia constant can be defined as the ratio of the kinetic energy of the rotor to the rated capacity of the synchronous generator at its rated speed, with the calculation formula as follows:

$$H_G = \frac{E}{S_{GN}} = \frac{J\omega_n^2}{2S_{GN}} \tag{1}$$

H_G is the inertia constant of the synchronous generator, with the unit of second (s); S_{GN} is the apparent power, with the unit of volt-ampere ($V \cdot A$); J denotes the moment of inertia, in units of kilogram-square meters ($kg \cdot m^2$); ω_n denotes the rated rotor speed, in units of radians per second (rad/s).

2.3. Inertia constant of photovoltaic power station

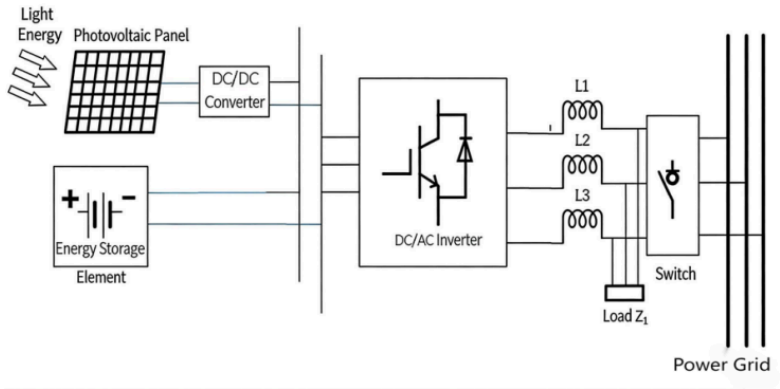

Figure 1. Electrical topology diagram of virtual synchronous generator in photovoltaic power station

Figure 1 illustrates the electrical topology of a virtual synchronous generator in a photovoltaic power station. As the system lacks rotating components and inherent rotational kinetic energy reserves, photovoltaic panels generate direct current (DC) that is fed into DC energy storage components via DC/DC converters. For analytical simplicity, the photovoltaic energy storage

DOI: 10.54254/2755-2721/2026.BJ32616

component is omitted, and the photovoltaic power station's generation capacity is assumed to be solely determined by the panel area, with its equivalent inertia constant set to zero.

2.4. Inertia constant of Doubly Fed Induction Generator

Doubly Fed Induction Generators (DFIGs) feature excellent variable-speed constant-frequency characteristics and are widely used in commercial wind power applications. Taking the inertia constant of a DFIG as an example, this paper analyzes the inertia constant of general wind turbines. These turbines normally operate in maximum power tracking mode. According to wind speed variations, the maximum power tracking curve can be divided into four distinct zones: startup zone, maximum power tracking zone, constant speed zone, and constant power zone, as illustrated in Figure 2.

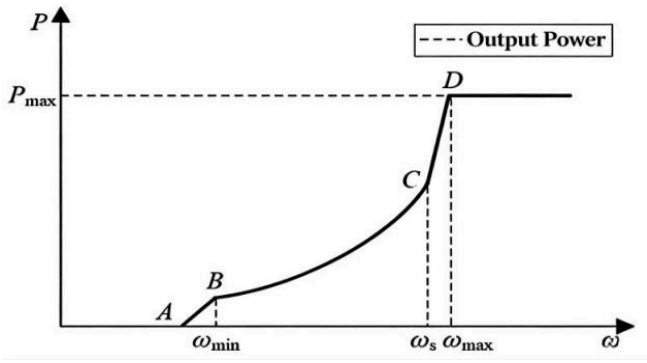

Figure 2. Maximum power tracking curve of a Doubly Fed Induction Generator

Depending on the actual operating conditions, the maximum power tracking curve of doubly fed induction generator is divided into the startup zone($\omega < \omega_{min}$),maximum power tracking ($\omega_{min} < \omega < \omega_s$),constant speed zone ($\omega_s < \omega < \omega_{max}$) ,constant power region ($\omega_{max} < \omega$).

The virtual equivalent inertia constant of doubly fed induction generator can be defined as the change of effective kinetic energy of doubly fed induction generator ΔE_k or the rated capacity of the equipment S_{wN} , lacks inertia response capability, with a virtual equivalent inertia constant of 0; when S_{wN} and $\omega_{max} < \omega$ assuming the wind turbine employs a maximum power tracking control strategy with uniform kinetic energy release during speed regulation, the virtual equivalent inertia constant of a doubly fed induction generator can be expressed as a function of wind speed v ,speed ω and output power P the only definite piecewise function is as follows:

$$H_w = \frac{1}{S_{wN}} \{ \frac{1}{2} J_w(\omega_0^2 - \omega_{min}^2) - \int_{t_{on}}^{t_{off}} \{ \frac{1}{2} \rho \pi R^2 C_{pmax} v^3 - 0.11 \rho \pi R^2 v^3 \cdot [116(\frac{v}{\omega R} - 0.035) - 5]e^{-12.5(\frac{v}{\omega R} - 0.035)} \} dt \} \tag{2}$$

$$H_w = \frac{1}{S_{wN}} \{ \frac{1}{2} J_w(\omega_{max}^2 - \omega_{min}^2) - \int_{t_{on}}^{t_{off}} 0.11 \rho \pi R^2 v^3 \cdot \{ [116(\frac{v}{\omega R} - 0.035) - 5] \cdot e^{-12.5(\frac{v}{\omega R} - 0.035)} - [116(\frac{v}{\omega R} - 0.035) - 5] e^{-12.5(\frac{v}{\omega R} - 0.035)} \} dt \} \tag{3}$$

Equation $\omega_{min} < \omega < \omega_{max}$ the expression of the virtual equivalent inertia constant of doubly fed induction generator; equation $\omega_{max} < \omega$ the virtual equivalent inertia constant expression of doubly fed induction generator is given.

DOI: 10.54254/2755-2721/2026.BJ32616

3. Unit combinational model with high proportion of asynchronous power sources

3.1. Object function

The unit combination problem is to minimize the power generation cost, which includes the coal consumption cost, the start-up cost and the shutdown cost.

$$min \sum_{i=1}^{N}(\sum_{i=1}^{T} C_i^f(P_{i,t}) + C_i^U + C_i^D) \tag{4}$$

$$C_i^f(P_{i,t}) = a_i {P_{i,t}}^2 + b_i P_{i,t} + c_i \tag{5}$$

In the formula, T is the number of scheduling periods; N is the number of generators; $P_{i,t}$ is the active power output of the i-th generator in the t-th period; C_i^f is the coal consumption cost of the i-th generator; C_i^U is the starting cost of the i-th generator; C_i^D is the shutdown cost of the i-th generator; a_i, b_i, and c_i are the quadratic, linear, and constant coefficients of the power generation cost function for the i-th generator, respectively.

3.2. Unit combination constraint

Solve the aforementioned objective function whilst incorporating constraints from conventional unit combination problems [5], including unit output constraints, power balance constraints, unit ramping constraints, system reserve constraints, minimum start-up/shutdown time constraints, start-up/shutdown cost constraints, and power flow safety constraints.

3.3. Model solving steps

In conclusion, the flowchart for optimal power flow calculation of the generation unit combination model incorporating high proportion of asynchronous power sources, as proposed in this paper, is illustrated below:

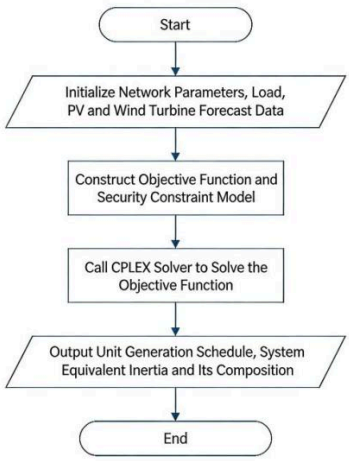

Figure 3. Flowchart of unit combination model solution

Step 1: Import network parameters, load, and pv/wind power forecast values.

DOI: 10.54254/2755-2721/2026.BJ32616

Step 2: Based on the model established above, construct the objective function and the set of safety constraints.

Step 3: Call the function with the constraint set as the feasible solution space cplex solver solves objective function

Step 4:Generate the generation plan, system equivalent inertia, and its composition scheme. From the perspective of power system operational safety, verify the constraint satisfaction of the optimization results. Combine the inertia assessment results to analyze the system's frequency stability support capability, thereby completing the scheme validity verification [6].

4. Case analysis

Matlab and Cplex Solver are employed to conduct optimal power flow calculations for the proposed high-proportion asynchronous power unit dispatch model on the IEEE 6-node system with wind and photovoltaic generation. Inertia assessment of the results verifies the optimized scheme's reliability. The system's frequency stability support capacity is analyzed based on inertia assessment results. Synchronous generators are located at Nodes 1, 2, and 3, with Node 1 as the slack node. For simplicity, wind and solar power offset the grid's total load without fixed grid connection points.

4.1. Output of synchronous unit in different periods

Using the system equivalent inertia model developed, the output power curves of synchronous units for each time period are generated by inputting load curves from each node, as shown in Figure 4.

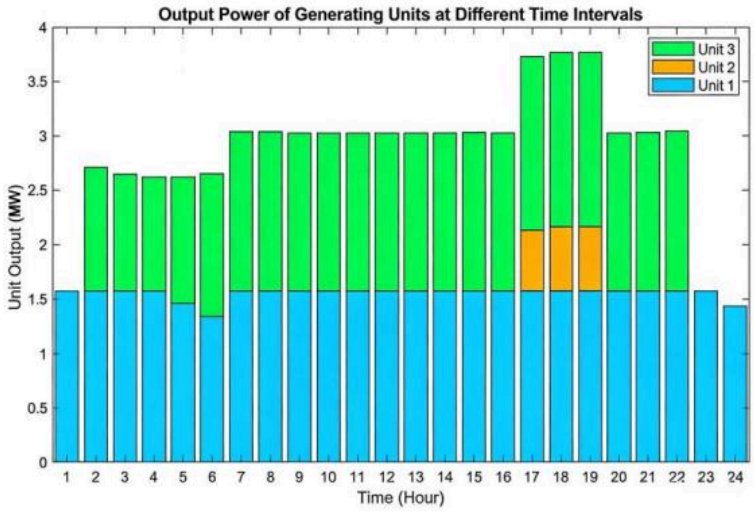

Figure 4. Output diagram of synchronous unit in different periods

Under the framework of coordinated optimization of unit dispatch and optimal power flow, the start-stop schedules and output levels of Units 1, 2, and 3 exhibit significant coupling responses with temporal fluctuations of the system load curve and output characteristics of renewable energy sources (wind/solar), consistent with the optimization logic of economic dispatch. These operational characteristics are highly compatible with the actual output patterns of renewable energy. When renewable energy output is insufficient and system load is high, synchronous units must increase their output to compensate for the renewable power deficit, meeting the power system's safety

DOI: 10.54254/2755-2721/2026.BJ32616

constraints and power balance requirements. This dispatch strategy effectively ensures the reliability and economy of system operation.

4.2. System equivalent inertia composition and proportion

As previously explained, photovoltaic power generation contributes zero to system inertia. The system's equivalent inertia comprises two components: rotational inertia from conventional synchronous generators and virtual inertia from wind turbines. Figure 5 illustrates the composition and comparison of these inertia components.

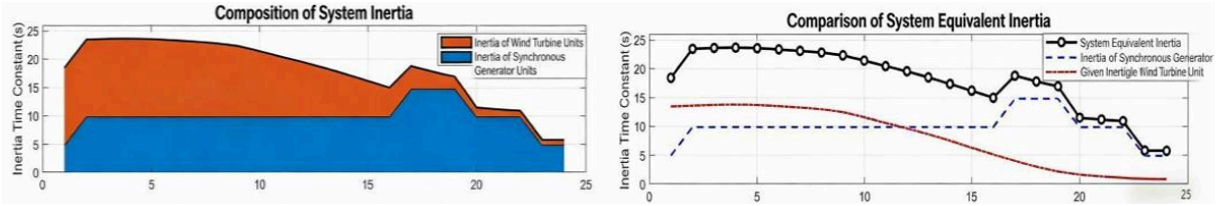

Figure 5. Comparison of system inertia composition

The temporal evolution of inertia characteristics shows that the equivalent inertia of synchronous units is strongly correlated with their output power distribution, reflecting robust coupling between inertia and operational status. In contrast, the virtual inertia of individual wind turbines declines sustainably over time, corresponding to their output characteristics: wind turbine output first decreases and then recovers in mid-periods. However, since virtual inertia's physical nature comes from integrating rotor kinetic energy and power fluctuations, output decline makes the corresponding power deficit integration term negative. This negative effect accumulates over time, ultimately keeping virtual inertia in a downward trend even after output recovery. This phenomenon reflects the "memory effect" of doubly fed induction generators' virtual inertia, indicating its level depends not only on current power status but also on the cumulative impact of historical power fluctuations, preventing synchronous recovery with instantaneous output changes.

5. Conclusion

To address reduced power system inertia and increased frequency stability risks from high-proportion asynchronous power grid integration, this study develops an improved generator set composition model considering both system equivalent inertia and diverse power source inertia characteristics. Its effectiveness is validated via a 3-generator 6-node system IEEE simulation case. Key findings: 1) A precise inertia evaluation model is established by analyzing multi-type power source inertia characteristics; 2) The equivalent inertia constant of photovoltaic power stations (without energy storage) is 0; 3) The piecewise expression of doubly fed induction generators' virtual equivalent inertia constant, influenced by operating conditions, accurately reveals its formation mechanism; 4) An integrated system equivalent model combining synchronous generators and wind turbines effectively resolves traditional methods' limitations in high-proportion asynchronous power integration scenarios.

By comprehensively considering synchronous units and doubly fed induction generators' inertia contributions, the model achieves efficient computation via linearization and the CPLEX solver. Simulation results show that compared to traditional combined unit models, the proposed model generates dispatching schemes that precisely respond to load and renewable energy output

DOI: 10.54254/2755-2721/2026.BJ32616

fluctuations, reducing system generation costs and effectively enhancing the system's equivalent inertia level to improve frequency stability.

With large-scale integration of high-proportion renewable energy, further validation is needed to evaluate photovoltaic energy storage virtual inertia contributions, coordinate multi-type inertia resource scheduling, and ensure engineering compatibility with larger-scale actual power grids.

References

[1] Sun Tongze. Research on Inertia Evaluation and Optimal Operation of New Power Systems [D]. North China Electric Power University (Beijing), 2024.
[2] Wen Yunfeng, Zhang Wuqi, Guo Wei. Inertia Demand of Power Systems: Concepts, Indicators and Evaluation Methods [J]. Automation of Electric Power Systems, 2024, 48(08): 30-41.
[3] Ba Wenlan. Research on Equivalent Inertia Prediction and Energy Storage Planning of Power Grids with High Proportion of Asynchronous Power Sources [D]. Hunan University, 2023.
[4] Lu Zongxiang, Jiang Jiheng, Qiao Ying, et al. Review on Generalized Inertia Analysis and Optimization of New Power Systems [J]. Proceedings of the CSEE, 2023, 43(05): 1754-1776.
[5] Zhang Wuqi, Wen Yunfeng, Chi Fangde, et al. Research Framework and Prospect of Power System Inertia Evaluation [J]. Proceedings of the CSEE, 2021, 41(20): 6842-6856.
[6] Lee , Y.-Y. , Baldick , et al. A Frequency-Constrained Stochastic Economic Dispatch Model [J].IEEE Transactions on Power Systems: A Publication of the Power Engineering Society, 2013, 28(3): 2301-2312.